INDIAN JOURNAL OF SCIENCE AND TECHNOLOGY

ORIGINAL ARTICLE

Large Language Model Based Prediction of SPT N value from Electrical Resistivity Correlations

N Karthik[1], S P Jeyapriya[2], M Rama[2]*

1 Department of Geotechnical Engineering, Government College of Technology, Coimbatore, Tamil Nadu, India
2 Department of Civil Engineering, Government College of Technology, Coimbatore, Tamil Nadu, India

OPEN ACCESS

Received: 25/07/2025

Accepted: 17/11/2025

Published: 15/12/2025

Citation: Karthik N, Jeyapriya SP, Rama M (2025) Large Language Model Based Prediction of SPT N value from Electrical Resistivity Correlations. Indian Journal of Science and Technology 18(46): 3640-3657. https://doi.org/10.17485/IJST/v18i46.1300

* **Corresponding author**.

mrama@gct.ac.in

Funding: None

Competing Interests: None

Published By Indian Society for Education and Environment (iSee)

ISSN
Print: 0974-6846
Electronic: 0974-5645

Abstract

Subsurface investigation and characterization of subsoil are the fundamentals for designing appropriate foundation systems for any Civil Engineering construction. Commonly employed geotechnical investigations are costly, laborious and time consuming whereas non-invasive methods like Electrical resistivity geophysical methods are widely used as it a low cost and fast technique used to identify subsoil strata. This method evaluates the apparent resistivity of soil from the measured resistance and used for characterization of subsoil strata. The aim of the present work is to identify the subsoil profile by measuring the resistivity of soil, establishing correlations between geoelectrical parameter and SPT N value thereby estimating the Safe Bearing Capacity (SBC) of soil. Multiple linear regression with interaction terms was employed using Large Language Model (LLM) to develop possible correlations between apparent resistivity and SPT N value. The study employed Electrical Resistivity geophysical method at selected locations complemented by borehole investigations to depths ranging from 0.0m to 12.0m. Borehole investigations were carried out at 19 locations using wash boring and conventional sounding tests like SPT to obtain the stiffness of soil at every 1.5m depth measured in terms of SPT N value. The resistivity values are integrated with borehole data to develop correlations, and the developed correlations predict SPT N using parameters such as depth, apparent resistivity, and interaction coefficients. Two electrode arrays namely Wenner and Schlumberger were used in this study. Among the two methods, the Schlumberger array showed higher resistance at 1.5m at all locations, while Wenner array gave higher resistance beyond 1.5m depth and the resistivity varied from 1.649Ωm to 246.176Ωm depending upon the soil types. Silty sand showed resistivity of 30.257Ωm whereas the presence of clay reduced the resistivity showing a minimum value of 19.97Ωm. Positive slopes showed increase in water content with respect to depth. It varied from 8.7% to 18.18% following increasing trend at location 15 but negative slope did not follow a definite pattern. There is no general relationship for correlating electrical resistivity and SPT N value for homogeneous soil layers and use of AI technique in establishing relationships has not been explored. The mathematical approach employed least squares optimization with depth resistivity interaction terms and zero-shot prompting technique to find relationships between geoelectrical and SPT N. The fitness of the model measured in terms of coefficient of correlation R^2 is observed as 0.9124.

Keywords: Electrical Resistivity; Standard Penetration Test; Wash Boring; Wenner; Schlumberger; Safe Bearing Capacity; Large Language Model

1 Introduction

Subsurface soils are extremely complex in nature, variable due to environmental conditions and are difficult to assess the characteristics of different layers. Subsurface investigation has evolved as a primary phase to be conducted before designing the substructure. Thorough investigations help in arriving at appropriate and cost-effective foundations for different structures. Investigations involve direct and semi-indirect methods that use vast instrumentation, time consuming thereby increasing the cost of investigation. Use of indirect geophysical methods such as electrical resistivity is a fast, non-destructive and less expensive method that has a high capability to predict geotechnical parameters. Many studies involved electrical resistivity to evaluate liquefaction of soil, detection of geomembrane failures, forecasting slope stability and bearing capacity of soil. Correlation between the values collected by the geophysical methods and the direct investigation techniques have been developed in recent years. Studies established correlations between electrical resistivity and hydraulic conductivity, electrical resistivity with variable water content, humus contents and salt contents. Correlations integrating Atterberg's limits, free swell index etc were also established. The Electrical Resistivity method is also widely employed in archaeological studies in unexcavated areas [(1)]. Its other uses include characterizing subsurface hydrogeology, determining the depth of bedrock or overburden thickness, identifying groundwater depth, mapping stratigraphy, delineating clay aquitards, detecting saltwater intrusion, assessing the vertical extent of specific soil and groundwater contamination, and estimating landfill thickness. Different subsoil shows different resistivity values and minimum values are observed when there is increase in clay content [(2)].

The present study was conducted with an idea of performing geophysical studies inorder to develop correlation equations with N-values for predominant soil identified at the investigation sites and classified as Poorly Graded Sand (SP) and Well Graded Sand (SW) as per IS classification system. Artificial Intelligent tool that can produce reliable results, largely reducing investigation time and costs has been employed for establishing correlation equations. This is the recent study that uses Large Language Models (LLMs) for developing apparent resistivity and SPT N relationships. Previous researchers have given correlation relationship for highly non-homogeneous soils showing limited focus on homogeneous types of soils with traditional empirical approaches. The novelty lies in AI-driven correlation development instead of conventional statistical methods. The difference between the previous studies and the present study is that correlations were developed for sedimentary and quaternary deposits [(3)], [(4)] and no correlations were developed for homogeneous soil of this particular type of soil.

The integration of geotechnical investigations and geophysical investigations in order to interpret the geological features in subsurface has been increasingly used. Wash Boring technique, a commonly employed technique for subsoil investigation, is used to advance boreholes and soil samples are collected at desired depths. It typically employs calyx equipment, mechanically driven by diesel engines to bore or drill through soil and rock. The Wash Boring technique was initially conducted complemented by Standard Penetration Test (SPT). It is performed at sites to determine the stiffness of soil measured as SPT N value. Split Spoon sampler is used to collect soil samples and a core catcher attached to the end of the drill bit is used to retrieve the cores. Field tests were conducted at 19 locations in and around Coimbatore, Tamil Nadu, India covering depths from ground level to borehole termination depth. Geophysical Electrical Resistivity was also conducted at all 19 study locations. This is a rapidly advancing technology that is gaining popularity for subsurface investigations. Electrical imaging not only identify subsoil stratigraphy but also effectively detects contamination in soil. Its versatility, supported by various electrode configurations, significantly shortens measurement time and makes it well suited for use in challenging and hard to reach uneven terrain. The Electrical Resistivity Meter operates using pairs of current and potential electrodes, the potential difference (V) is measured using the potential electrodes, while the current (I) is introduced into the ground through the current electrodes. According to Ohm's law, $V = I \times R$ since V and I are known, the resistance (R) can then be calculated.

Electrical Resistivity values are critical for understanding soil behaviour and are considered as essential soil parameters for geotechnical analysis, such as stability, strength, and safe bearing capacity. The behaviour of electrical current flow in subsurface soil indicates that the relationship between soil strength and electrical resistivity depends on factors such as grain size distribution, saturation level, porosity [(2)]. Observations from the electrical resistivity meter indicate that saturated soil exhibits higher conductivity, with reduction in electrical resistance. It is therefore essential to understand the importance of geophysical investigation using electrical resistivity tomography to determine the spatial extension of underground cavities[5]. Integration of geophysical and geotechnical methods helps in the identification of geologic strata. The geotechnical data included standard penetration test soundings and soil characterization[6].

The present study uses two different electrode configurations, namely the Wenner and Schlumberger arrays. The resistivity values reflect varying geological formations that comprise the subsurface structure[7]. Large Language Model was used to develop correlation using 94 datasets that relate resistivity measurements and SPT N-values, enabling the assessment of safe bearing capacity using established equations for two different classifications of Sand. It provides optimal linear regression equations, leveraging artificial intelligence capabilities to identify complex patterns and generate precise predictive models that enhance the accuracy of the correlation relationships. The derived relationships provide engineers with an efficient approach for foundation design by integrating geophysical data for bearing capacity calculations.

2 Methodology

2.1 Field Investigation

Field investigations were carried out through geotechnical and geophysical assessments utilizing the Standard Penetration Test and Electrical Resistivity geophysical Test. Laboratory analysis such as sieve analysis and Atterberg's limits were performed following standard procedure. The Standard Penetration Test (SPT) is a widely utilized field test in geotechnical engineering, primarily designed to evaluate the safe bearing capacity (SBC) of soil. The N-value obtained from the SPT represents the resistance to penetration of soil and can be correlated with its compaction, density, and strength. These values are subsequently applied in calculations to estimate the SBC, defined as the maximum load per unit area that the soil can sustain without failure.

2.2 Wash Boring

Wash boring stands out as the most frequently employed boring technique among all available drilling methods. The initial equipment setup duration varies based on specific site conditions. The drilling process begins to create boreholes in the ground. Throughout the drilling operation, a circulating fluid typically bentonite slurry is used to serve multiple purposes. This fluid helps dissipate the heat generated during the drilling process, thereby protecting the core bit from thermal damage. Additionally, the circulating fluid acts as a stabilizing agent, providing structural support to the borehole walls and preventing soil collapse into the excavated hole.

2.3 Electrical Resistivity

The electrical resistivity equipment used is the AQUAMETER CRM (Computerized Resistivity Meter) AUTO C, the latest version of CRM. This advanced model automatically select the ground current based on the ground conditions, enhancing user convenience by eliminating the need to manually adjust the current value. Starting with a minimum current of 1mA, the instrument incrementally increases the current until it reaches the maximum permissible value for the specific field conditions. It measures the potential difference between the potential electrodes and calculate the resistance, considering the current sent by the device. The Wenner and Schlumberger methods are employed to determine the apparent resistivity (Ωm) of the soil with respect to spacing of electrodes whereas the depth of current penetration below the ground surface is approximately equal to spacing of electrodes[8]. The accuracy of the measured data is largely influenced by the contact between the electrodes and the ground. Favourable conditions for measurements include natural ground, uniform clay profiles, thin surface layers, and relatively wet conditions. In contrast, factors that reduce measurement quality include fill materials, pavements, coarse soil layers, low ground water tables and thick dry surface crusts. Two-dimensional resistivity measurements provide a continuous and, ideally when paired with other geophysical techniques like reflection seismic and ground-penetrating radar, a relatively detailed view of the subsurface in a short time. In areas with no prior investigations, the 2D resistivity method offers an overview of the subsurface, serving as a foundation for further studies and helping to determine the best locations for drilling. 2.5D ERT survey could identify open fractures and cavities at accurate locations along with its rough size and shape[9]. Electrical resistivity imaging revealed significant variability in the near-surface materials and identified the presence of impermeable layers that may define the horizontal and vertical boundaries of permeable zones.

2.4 Wenner Method

The Wenner configuration consists of four electrodes arranged in straight line, evenly spaced and symmetrical about a central point, with an additional reference electrode buried in the ground. The resistance of the soil beneath this reference electrode is measured and remain fixed throughout the test. The electrodes are typically buried at a depth of 10cm to 15cm below the natural ground level. The two outer electrodes A and B, function as current electrodes, while the two inner electrodes M and N, serve as potential electrodes. The arrangement of electrodes for this configuration is represented in Figure 1(a). Among the various electrode arrays used in electrical resistivity testing, the Wenner configuration is one of the simplest to calculate the apparent resistivity and during every new measurement, all the electrodes must be repositioned for each new resistance reading.

This configuration does not require additional correction factors in its calculations for apparent resistivity. The resistivity of subsurface layers is determined by progressively increasing the distance between the electrodes while keeping the central point of the array stationary. The Vertical Electrical Sounding (VES) examines variations in the resistivity of layers of earth in the vertical direction. VES also known as electrical drilling or expanding probe technique, is extensively used in geotechnical studies where readings are taken as current reaches greater depths(10).

2.5 Schlumberger Method

The Schlumberger configuration employs the same number of electrodes as the Wenner configuration, but the key difference lies in the spacing of the electrodes. In this setup, the resistance of the soil is measured beneath the reference electrode. This method is simpler for field investigations because the potential electrodes remain fixed, while only the current electrodes are moved. The spacing between the potential electrodes is denoted as 2l, and the spacing between the current electrodes is denoted as 2L where l and L are respectively the distance from the reference electrode to potential electrodes and the distance from reference to current electrodes. The array configuration of this method is shown in Figure 1(b).

In this configuration, the current electrodes are positioned farther away from the potential electrodes. The Schlumberger array typically offers better resolution and requires less time for field deployment compared to the Wenner array. The Schlumberger configuration is easier to implement in the field, it can be challenging or confusing for persons to carry out the investigation due to its spacing requirements(11). The calculation process is also more complex compared to the Wenner, as it involves determination of spacing factor (K) for each measurement.

2.6 Study area and classification of soil from borehole investigations

The investigation encompassed a spatial framework spanning Coimbatore and Tiruppur districts. A total of 19 locations were selected, and borehole soil investigation works were carried out at all the locations for a comprehensive study. The geographical distribution is depicted in Figure 2.

Electrical resistivity was conducted at the same location and at all borehole points. At certain locations, more than one borehole point was selected depending on the extent of area. Soil samples extracted through wash boring technique were subjected to detailed laboratory examination to find the properties and the classification of soil as per BIS classification system. The locations of test conducted along with soil types are presented in Table 1. This integrated approach combining geophysical testing with direct sampling methods provided a thorough understanding of subsurface conditions across the study region. Only the depths mentioned against each location has shown collection of soil samples. At the last 6 locations (locations 14 to 19), below Poorly Graded Sand/Well Graded Sand, soft rock is encountered. As most of the collected samples are classified as Well Graded Sand (SW) and Poorly Graded Sand (SP), correlation equations are developed for these two of soil types to predict SPT-N values and SBC.

2.7 Data Processing

Field investigations of electrical resistivity measure the observed resistance in ohm(Ω) and this parameter is used to calculate the apparent resistivity of the soil in ohm-meter (Ωm). Apparent resistivity is a calculated value that reflects the overall electrical resistance of the soil, influenced by factors such as soil type, moisture content, unit weight and the electrode configuration. Apparent resistivity for the Wenner array(10) is calculated using **Eqs. (1) and (2).**

$$\rho_a = 2\pi aR \tag{1}$$

$$R = \{\frac{\Delta v}{I}\} \tag{2}$$

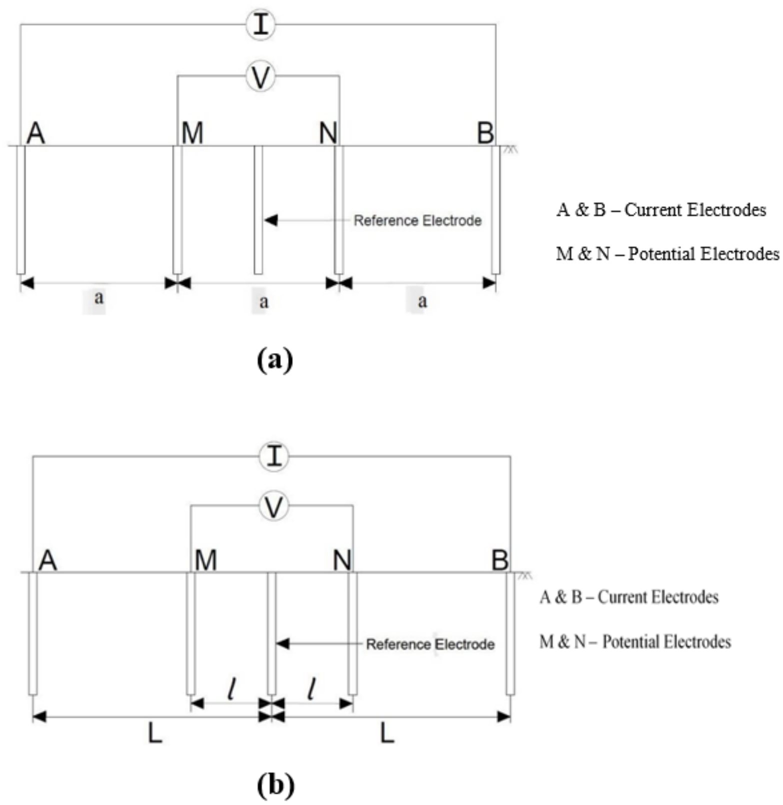

Fig 1. Wenner and Schlumberger Array Configurations

Where,

ρ_a is apparent resistivity (Ωm), a is spacing between adjacent electrodes (m), Δv is potential drop, I is applied current and R is observed resistance (Ω)

Schlumberger array used **Eqs. (3), (4) and (5)** to determine the resistivity of soil[10].

$$\rho_a = \frac{\pi L^2}{2l}\frac{\Delta v}{I} \tag{3}$$

The equation can be simplified as,

$$\rho_a = K \times R \tag{4}$$

$$K = (l|2)[\{L|l\}2 - 1] \tag{5}$$

Where,

K is spacing factor, l is the distance from reference electrode to potential electrodes and L is distance from the reference electrode to current electrodes, Δv is potential drop, I is applied current and R is observed resistance (Ω).

Field investigations using electrical resistivity equipment yielded apparent resistivity measurements corresponding to electrode spacing. These apparent resistivity data, together with their respective electrode spacing parameters, were subsequently processed through Res2DInv inversion software (Loke and Barker, 1996) to derive true resistivity values as a function of depth[12]. The inversion program divides the subsurface into small rectangular blocks. The program automatically generates the blocks and finite element modelling is used to calculate the apparent resistivity at a particular location.

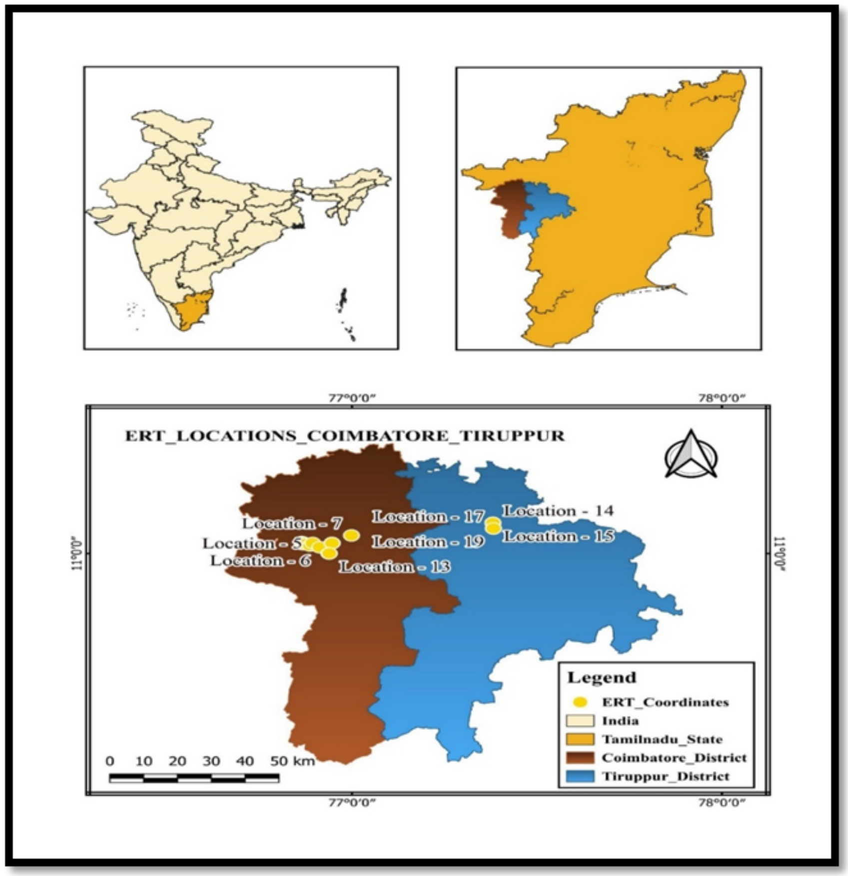

Fig 2. Electrical Resistivity Test locations

2.8 Safe Bearing Capacity

Safe Bearing Capacity serves as a fundamental parameter explaining the bearing capacity of soil and is essential for designing of foundations for any type of structure. Multiple geotechnical parameters govern SBC evaluation, encompassing Standard Penetration Test N-values, soil density characteristics, soil type, and expected settlement patterns that vary according to specific soil engineering behaviour. Bearing capacity evaluation based on shear criterion and settlement criterion is presented in **Eqns. (6) and (7)** proposed by Teng[(13)].

Bearing Pressure corresponding to Shear Failure criterion:

The ultimate bearing capacity, q_u with a factor of safety of 3 is given by

$$q_u = 2N^2 \cdot B \cdot W_q + 6(100 + N^2) \cdot D_f \cdot W_\gamma \tag{6}$$

Where,

N is Number of blows, D_f is Depth of foundation (m), B is Minimum size of the foundation, W_q and W_γ are Water table correction factors (for the worst case taken as 0.5)

Bearing Pressure corresponding to Settlement consideration:

The safe bearing pressure (Allowable bearing pressure), q_s (in kN/m^2) corresponding to the permissible settlement is given by

$$q_s = 1.36(N - 3) \times \{(B + 0.3)/2B\}^2 S \cdot R_d \cdot R_w \tag{7}$$

Where,

B is the Maximum size of the footing (m), S is Permissible differential settlement (mm),

R_d is Depth factor, and R_w is Water table correction factor (for the worst case, taken as 0.5)

Table 1. Locations of Electrical Resistivity Test and Borehole investigations

Sl. No.	Locations	Depth (m)	IS Classification	Depth of termination of Borehole (m)
1	Location - 1 Podhigai Residency	0.0 - 4.5	Well Graded Sand (SW)	4.5
2	Location - 2 Ganapathy Nagar	0.0 - 1.5	Poorly Graded Sand (SP)	4.5
		1.5 - 4.5	Well Graded Sand (SW)	
3	Location - 3 Kamatchi Nagar	0.0 - 6.0	Poorly Graded Sand (SP)	6
4	Location - 4 Vijay Nagar	0.0 - 3.0	Low Compressible Clay (CL)	5
		3.0 - 5.0	Poorly Graded Sand (SP)	
5	Location - 5 Nanjappa Nagar	0.0 - 5.0	Poorly Graded Sand (SP)	5
6	Location - 6 Vadavalli	0.0 - 8.0	Well Graded Sand (SW)	8
7	Location - 7 Saravanampatti	0.0 - 1.5	Clay (C)	12
		1.5 - 12.0	Poorly Graded Sand (SP)	
8	Location - 8 Kavundampalayam BH-01	0.0 - 1.5	Filled up Soil	5.50
		1.5 - 4.0	Well Graded Sand (SW)	
		4.0 - 5.5	Silty Sand (SM)	
9	Location - 9 Kavundampalayam BH-02	0.0 - 1.5	Filled up Soil	5
		1.5 - 3.0	Poorly Graded Sand (SP)	
		3.0 - 5.0	Silty Sand (SM)	
10	Location -10 Kavundampalayam BH-03	0.0 - 3.0	Poorly Graded Sand (SP)	5
		3.0 - 4.0	Intermediate Compressible Clay (CI)	
		4.0 - 5.0	Poorly Graded Sand (SP)	
11	Location - 11 Chokampudur BH-01	0.0 - 1.5	Well Graded Sand (SW)	4
		1.5 - 4.0	Poorly Graded Sand (SP)	
12	Location - 12 Chokampudur BH-02	0.0 - 1.5	Well Graded Sand (SW)	4
		1.5 - 4.0	Well Graded Gravel (GW)	
13	Location - 13 Chokampudur BH-03	0.0 - 5.0	Poorly Graded Sand (SP)	5
14	Location - 14 Kasipalayam BH-01	0.0 – 9.0	Poorly Graded Sand (SP)	9
15	Location - 15 Kasipalayam BH-02	0.0 - 9.0	Poorly Graded Sand (SP)	9
16	Location - 16 Kasipalayam BH-03	0.0 - 8.0	Well Graded Sand (SW)	8
17	Location - 17 Rakiyapalayam BH-01	0.0 – 9.0	Well Graded Sand (SW)	9
18	Location - 18 Rakiyapalayam BH-02	0.0 - 9.0	Poorly Graded Sand (SP)	9
19	Location - 19 Rakiyapalayam BH-03	0.0 - 9.0	Poorly Graded Sand (SP)	9

2.9 Large Language Model

Large Language Model (LLM) is an artificial intelligence system that learns from extensive text collections to comprehend and produce natural language. Through transformer architectures, these models acquire the ability to execute various functions by identifying patterns within massive textual datasets during their training process. Zero shot prompting is an approach applied in situations where no previous examples or references exist to guide the task and followed by Supervised learning such a method is utilized for prediction of N-values. LLM has recently exhibited remarkable proficiency across various domains, encompassing the understanding of natural language. LLM has the capacity to comprehend intricate linguistic structures and produce contextually relevant and coherent responses tailored to specific scenarios. LLMs create an impact to society and shape the future of AI to solve real world problems[14] and suitability of corresponding computational intelligence algorithms for constructing the resistivity map are emerging as open research areas[15].

The LLM Claude 3.5 Sonnet executed the correlation development through a systematic four-stage process within its transformer-based, decoder-only architecture utilizing multi-head self-attention mechanisms in the present research. Initially, the Statistical Analysis Module performed regression modeling on the input datasets (ERT resistivity ρ, SPT N-values, and depth D), analyzing their statistical relationships and distributions. This is followed by the Pattern Recognition Module detecting correlations between variables using attention layers to understand how depth and resistivity jointly influence SPT N-values, recognizing both direct and interaction effects. The next module called, the Equation Formulation Module synthesized these findings to construct the multivariate linear regression model $N = a + b_1 D + b_2 \rho + b_3 (D \times \rho)$, optimizing the coefficients (a, b_1, b_2, b_3) to best fit the field data. Finally, the Validation Metrics Module calculated comprehensive statistical measures including R^2 to quantify the accuracy of predictive equations. The working flow of LLM architecture is shown in Figure 3.

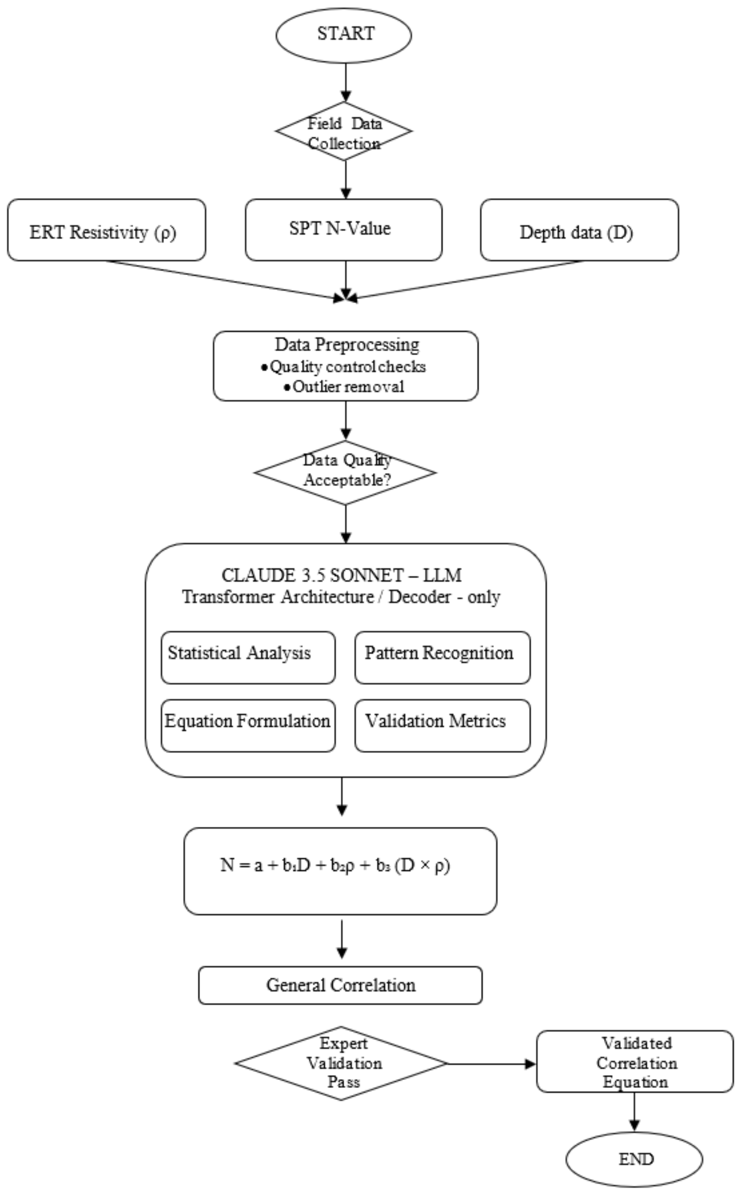

Fig 3. LLM - Architecture

2.10 Comparative analysis of electrode arrays

Field observations and the calculated apparent resistivity showed that at 1.5m depth, Schlumberger array showed higher observed resistance than Wenner but beyond 1.5m, the latter method gave higher observed resistance. Wenner array showed a consistent pattern at 3m depth, and the observed resistance was between 1/2 and 1/3 of the resistance observed at 1.5m, but this pattern was not seen in Schlumberger array. Both Wenner and Schlumberger arrays failed to give any readings when electrode spacing was 0.5m. Observed resistance values decreased when electrode spacing increased. Table 2 represents the resistivity observed for different types of soil at the selected locations.

Table 2. Soil types and Range of Apparent Resistivity using Wenner and Schlumberger Array methods

Sl. No.	Type of soil	Range of Apparent Resistivity (Ωm) (Wenner Array)	Range of Apparent Resistivity (Ωm) (Schlumberger Array)
1	Well Graded Gravel (GW)	3.203 - 4.522	1.649 – 3.018
2	Well Graded Sand (SW)	2.204 – 141.300	2.393 – 246.176
3	Poorly Graded Sand (SP)	2.939 – 83.650	2.419 – 125.600
4	Silty Sand (SM)	30.257 – 55.955	34.191 – 67.643
5	Clay (C)	23.738 – 79.505	19.970 – 86.386

At the same measurement sites, an inverse relationship was observed between moisture content and apparent resistivity when plotted against depth. A negative slope in apparent resistivity corresponds to a positive slope in moisture content, indicating an inverse relationship; conversely, an increase in apparent resistivity (positive slope) was associated with a decrease in moisture content (negative slope). The negative apparent resistivity trend corresponds to positive moisture content values that progressively rise from surface levels to greater depths. The type of slope can be used to predict moisture content patterns. Studies of Self Potential survey displayed that positive values identified locations of water discharge and negative values are seen in the sites of infiltration[(16)].

2.11 Correlation between Electrical Resistivity and SPT N-value

The electrical resistivity testing conducted using the Wenner array demonstrated better performance compared to the Schlumberger array. This advantage prompted the development of correlation equations to predict SPT N-values from electrical resistivity measurements.

The Standard Penetration Test (SPT) yields an output called the N-value, representing the number of hammer blows needed to drive the sampler to 30cm into the soil excluding the first 15cm penetration that is considered as seating drive. This observed N-value cannot be used directly for SBC calculations and corrections must be applied to obtain the Corrected N-value and this value is used in Teng's equation to determine the SBC of soil.

Through wash boring and SPT procedures, soil samples are retrieved from all 19 testing locations and all collected soil samples are subjected to laboratory analysis for soil classification purposes. This classification process enabled data grouping based on soil type. The investigation yielded 51 data points for Poorly Graded Sand (SP) and 27 data points for Well Graded Sand (SW).

Through linear regression analysis, mathematical equations were developed to predict both observed and corrected N-values specifically for the Wenner array configuration. The general form of the relationship is given in **Eq. (8)**. This is a multiple linear regression model predicting SPT-N values using depth (D) and Wenner apparent resistivity. The model includes an interaction term (D $\times$ ρ) to capture combined effects of depth and resistivity on soil strength. Regression coefficients a, b_1, b_2, b_3 are dimensionally adjusted to ensure the final SPT-N, a dimensionless data, enabling geotechnical prediction of N-value without extensive drilling.

$$N = a + b_1 D + b_2 \rho + b_1 (D \times \rho) \quad (8)$$

Where,

N is (observed) N-value, D is Depth (m), ρ is Wenner Apparent Resistivity (Ωm), D $\times$ ρ is interaction term between depth and resistivity (Ωm^2), a, b_1, b_2, b_3 are regression coefficients, a is intercept coefficient, b_1 depth coefficient, b_2 resistivity coefficient, b_3 interaction coefficient.

3 Results and Discussion

Both borehole and Electrical Resistivity Geophysical tests were carried out at all the study locations by employing wash boring for Borehole investigation and Wenner and Schlumberger arrays for geophysical methods. SPT tests were carried out at every 1.5m depth and sampling was done using Split spoon sampler. Figures 4(a) and (b) illustrate the positive and negative slope patterns observed in the Wenner array measurements. The positive slope pattern indicates that the depth and apparent resistivity are directly proportional, and the negative slope indicates the vice versa relationship among the two. Similarly, Figures 4(c) and (d) depict the positive and negative slope patterns of Schlumberger method.

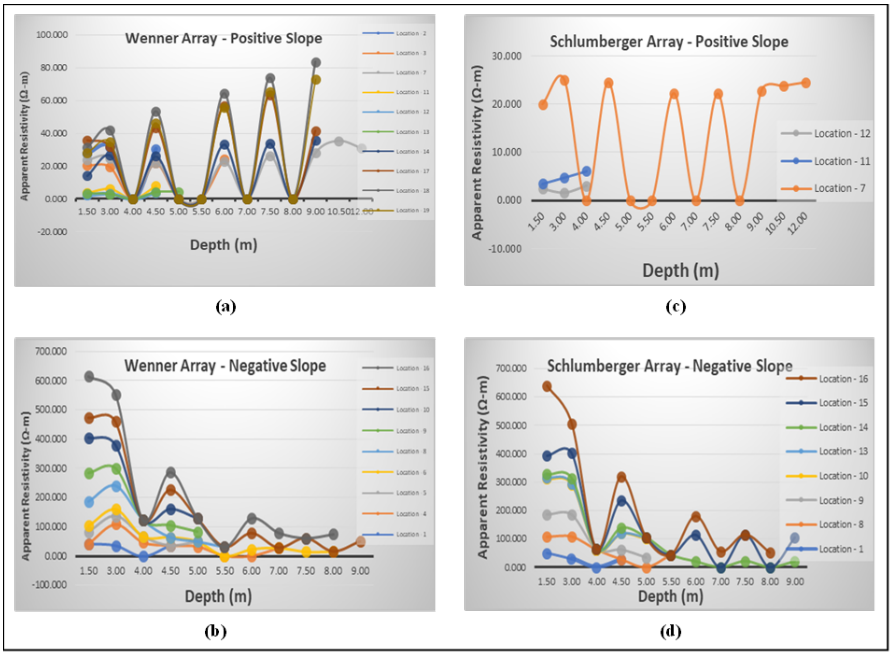

Fig 4. Positive and Negative Slopes of Wenner and Schlumberger Array

Comparing average R^2 values obtained from both these methods revealed that, Wenner method performs better than Schlumberger approach, representing the effectiveness of former method. Hence, most of the experimental work on site was done using Wenner method of electrical resistivity.

The geophysical mapping of subsurface features can provide information about the spatial distribution of physical properties, such as electrical conductivity (or resistivity)[17]. Referring to resistivity values, Well Graded Gravel (GW) exhibited relatively low apparent resistivity attributed to the presence of large voids between the particles hindering the flow of electric current. In contrast, Well Graded Sand (SW) showed higher resistivity due to densely packed structure, facilitating the movement of electricity more efficiently, on the surface of dry sands the resistivity is high[18]. Soil with high porosity contains large quantities of water, results in a low field ERV. Conversely, denser soil increases the field ERV due to its lower void ratio and reduced porosity. The natural water content of soil has a strong correlation with electrical resistivity indicating that increase in water content results in a decrease in electrical resistivity[19].

The observed resistance consistently followed a descending order as the depth increased, but the same pattern was not observed in the apparent resistivity. The Wenner array showed higher coefficient of determination than the Schlumberger array, making it more suitable to establish correlation with SPT N-values. A source of error arises when the friction at the rod tip varies significantly. For Poorly Graded Sand (SP) the apparent resistivity ranged from 2.939Ωm to 125.600Ωm, while for Well Graded Sand (SW), it varied from 2.204Ωm to 246.176Ωm. In case of SW, the given range of values are at 1.5m depth but the difference in the apparent resistivity value is due to moisture content, density and compactness of the soil at site. Electrical Resistivity Tomograph is used to obtain geological subsurface imaging. It is also used for the determination of water bearing strata that showed decreased electrical resistivity[20]. Table 3 illustrates the slope categories and the corresponding moisture content along with apparent resistivity for few study locations.

Well Graded Gravel (GW) was observed only at one site, with apparent resistivity varying from 3.203Ωm to 4.522Ωm. whereas for Silty Sand (SM), the same ranged between 30.257Ωm and 55.955Ωm. Coarse grained particles have more voids when

Table 3. Slope classification based on moisture content for few study locations

Sl. No.	Depth (m)	Locations	Type of Slope	% of moisture content (W)	Apparent Resistivity (Ωm)
1	0.0 - 1.5	15	Positive	8.7	68.012
2	1.5 - 3.0			10.87	80.07
3	3.0 - 4.5			12.24	64.715
4	4.5 - 6.0			14.29	54.636
5	6.0 - 7.5			17.5	46.817
6	7.5 - 9.0			18.18	49.285
7	0.0 - 1.5	16	Positive	15.63	141.3
8	1.5 - 3.0			18.18	93.823
9	3.0 - 4.5			19.35	61.042
10	4.5 - 6.0			19.44	51.245
11	6.0 - 7.5			20	51.301
12	7.5 - 8.0			24.95	59.283
13	0.0 - 1.5	17	Negative	12.96	35.796
14	1.5 - 3.0			11.67	31.84
15	3.0 - 4.5			11.11	43.52
16	4.5 - 6.0			10.42	56.897
17	6.0 - 7.5			11.11	63.585
18	7.5 - 9.0			11.76	41.542
19	0.0 - 1.5	18	Negative	19.67	31.557
20	1.5 - 3.0			17.07	41.825
21	3.0 - 4.5			19.7	53.411
22	4.5 - 6.0			18.97	64.433
23	6.0 - 7.5			20.37	73.947
24	7.5 - 9.0			15.63	83.65
25	0.0 - 1.5	19	Negative	17.65	27.977
26	1.5 - 3.0			16.98	34.666
27	3.0 - 4.5			12.2	46.346
28	4.5 - 6.0			16.98	55.766
29	6.0 - 7.5			15.91	65.469
30	7.5 - 9.0			12.77	72.911

compared to fine grained particles, due to the voids in coarse grained particles the flow of current was hindered. These voids facilitate the movement to water freely which increases the flow of current and in such condition, it leads to lesser resistivity[21]. The developed correlation equation and the application of this equation is dependent on the specific soil types investigated in this study and may not be applicable to other soil classifications beyond these types of soil. Additionally, the predictive accuracy of the equation is restricted to a depth range of 1.5m to 9.0m, and extrapolation beyond this range may result in unreliable predictions.

The classification of slopes into positive and negative categories is fundamentally dependent on moisture content distribution characteristics. Positive slope occurs when moisture content demonstrates an increasing pattern as depth extends downward from the surface level and the trend of apparent resistivity in the decreasing order whereas negative slope follows increasing trend of apparent resistivity measurements. ERT creates discrete subsurface images at various depths and further interpolated into continuous 2D tomograms showing electrical resistivity variations that reveal lithological and water content changes. 2D resistivity tomographies integrated with geological and geotechnical data is useful to find different layers[22]. Lithologic variations both in lateral and vertical directions are studied using 2D ERT inversions[23]. Subsurface images interpolated into tomograms using Res2DInv inversion software uses finite element modelling to calculate the apparent resistivity, and this can be suited for Wenner Schlumberger arrays. The output showed variation in resistivity that revealed different strata. An ERT obtained for site location 14 is shown in Figure 5. It is observed that apparent resistivity is same as true resistivity for homogeneous layers. The apparent resistivity is different from true resistivity unless the subsurface materials are homogeneous [10]. Figures 6 and 7 demonstrate the slope categories and the corresponding moisture content as well as the apparent resistivity. The graphical results for the final five locations are presented due to their close geographic proximity to one another.

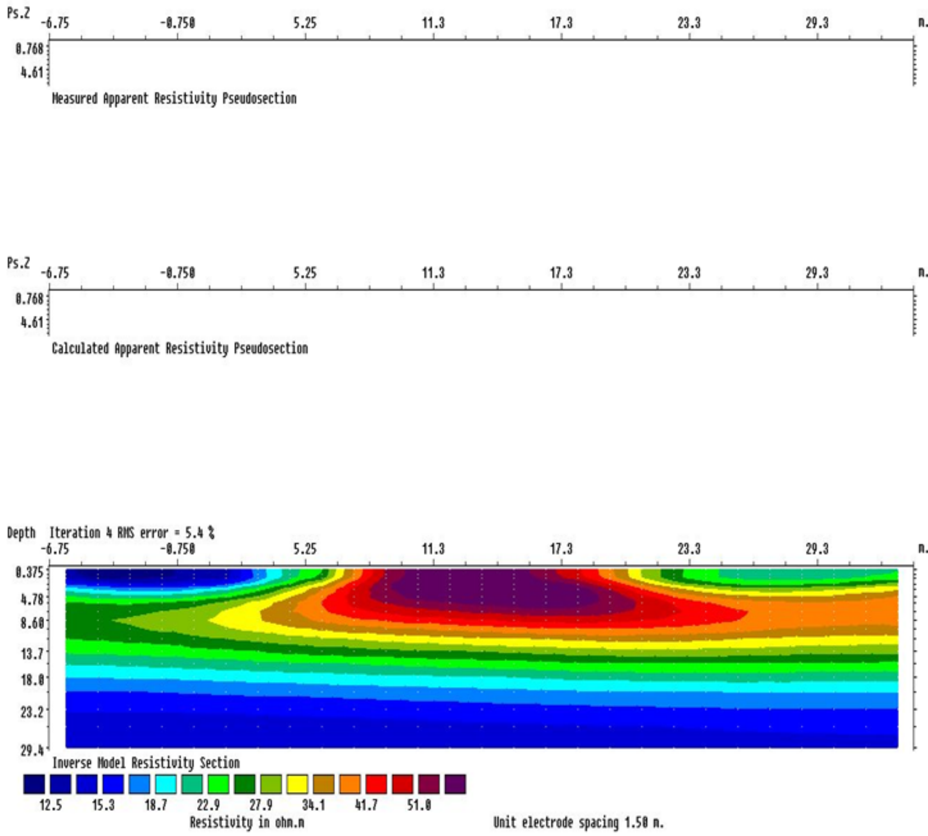

Fig 5. Electrical Resistivity Tomogram (Location 14)

Data prediction was achieved by utilizing extensive datasets as input parameters, from which corresponding outputs were predicted. This approach functions as an empirical modelling technique that establishes relationships between input variables and predicted outcomes based on observed data patterns. The employment of LLM technology for empirical relationship development successfully transformed raw geotechnical investigation data into mathematically coherent predictive models through pattern analysis and statistical computation techniques. The methodology exhibited better performance in rapid dataset processing, implementation of complex regression analyses incorporating multiple variable interactions, and effective integration of fundamental geotechnical engineering principles from comprehensive knowledge databases. The zero-shot prompting methodology proved particularly valuable in establishing empirical correlations to specific site conditions. **Equations 9 and 10** present the correlation equations for predicted N value (N_p) for Well Graded Sand (SW) and Poorly Graded Sand (SP) respectively.

$$N_p = 22.45 + 4.87 \times D + 0.145 \times \rho - 0.018 \times D \times \rho \tag{9}$$

$$N_p = 32.85 + 2.12 \times D + 0.089 \times \rho - 0.021 \times D \times \rho \tag{10}$$

Studies conducted by Roodposhti et.al. (2019) suggested polynomial relationship between electrical resistivity, water content and compaction in the field [3]. Variable parameters that effect electrical measurements are the gradation of soil and spacing of electrodes. Relationships established by studies in the evaluation of N value are useful to determine the stiffness of soil and

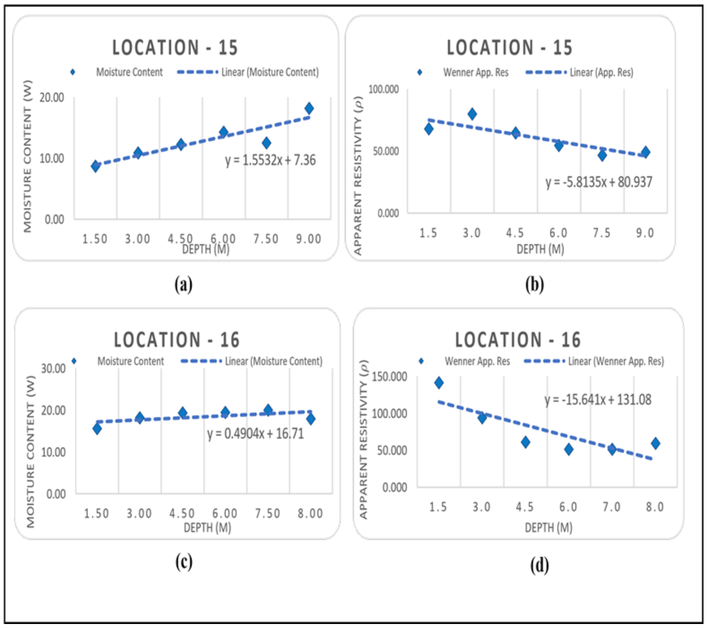

Fig 6. Positive Moisture Content and Negative Apparent Resistivity Slopes

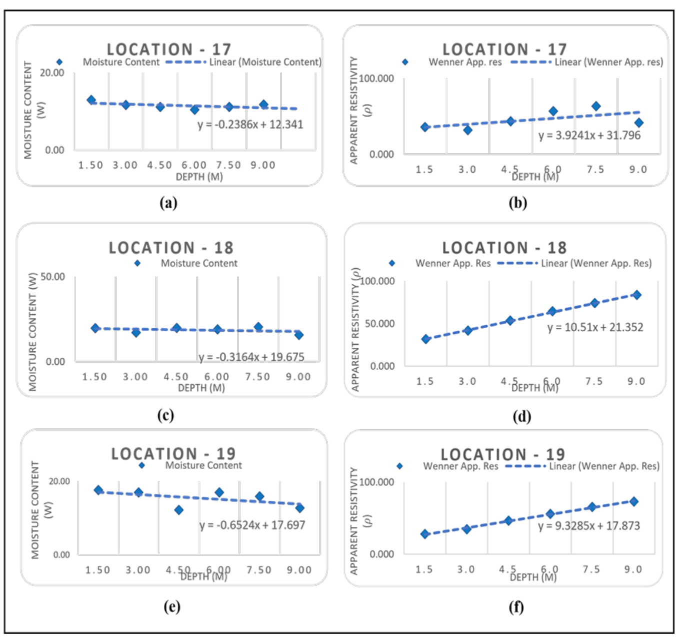

Fig 7. Negative Moisture Content and Positive Apparent Resistivity Slopes

other geotechnical properties that are valuable for foundation design and engineering design of earth retention systems. The observed N-values obtained from borehole data and the predicted N using correlation equations are shown in Table 4.

Table 4. Observed and Predicted N-values for Well Graded Sand and Poorly Graded Sand

Sl. No.	Loca-tions	Depth (m)	Apparent Resistivity (Ωm)	Observed N-Value (Experiment)	Predicted N- Value (LLM)	Sl. No.	Loca-tions	Depth (m)	Apparent Resistivity (Ωm)	Observed N-Value (Experiment)	Predicted N- Value (LLM)
Well Graded Sand (SW)						13	7	3.0	24.869	50	40
1	1	1.5	41.260	13	35			4.5	21.845	>50	42
		3.0	35.608	34	40			6.0	22.683	>50	45
		4.5	35.890	38	47			7.5	26.376	>50	47
2	2	3.0	31.651	24	40			9.0	27.977	>50	49
		4.5	30.493	50	46			10.5	35.278	>50	50
3	6	1.5	21.007	13	32			12.0	30.973	>50	53
		3.0	22.796	27	39	14	9	3.0	60.288	26	41
		4.5	28.514	32	46	15	10	1.5	121.518	17	43
		6.0	23.249	48	53			3.0	79.505	20	41
		7.5	14.318	>50	59			5.0	46.786	59	43
		8.0	15.072	>50	61	16	11	3.0	6.293	50	39
4	8	3.0	79.882	17	44			4.0	8.064	>50	41
		4.0	56.520	59	46	17	13	1.5	3.335	13	36
5	11	1.5	3.721	29	30			3.0	2.939	50	39
6	12	1.5	2.204	26	30			4.0	4.041	>50	41
7	16	1.5	141.300	50	46			5.0	4.365	>50	43
		3.0	93.823	>50	46	18	14	1.5	14.130	>50	37
		4.5	61.042	>50	48			3.0	26.564	>50	40
		6.0	51.245	>50	54			4.5	25.971	>50	42
		7.0	51.301	>50	58			6.0	33.196	>50	44
		8.0	59.283	>50	61			7.5	33.865	>50	46
8	17	1.5	35.796	50	34	19	15	1.5	68.012	>50	40
		3.0	31.840	49	40			3.0	80.070	>50	41
		4.5	43.520	>50	47			4.5	64.715	>50	42
		6.0	56.897	>50	54			6.0	54.636	>50	44
		7.5	63.585	>50	60			7.5	46.817	>50	46
		9.0	41.542	>50	66			9.0	49.285	>50	47
Poorly Graded Sand (SP)						20	18	1.5	31.557	45	38
9	2	1.5	27.695	50	38			3.0	41.825	>50	40
10	3	1.5	20.441	18	37			4.5	53.411	>50	42
		3.0	19.330	18	40			6	64.433	>50	43
		4.5	21.732	50	42			7.5	73.947	>50	44
		6.0	24.492	>50	45			9.0	83.650	>50	44
11	4	4.0	32.584	22	41	21	19	1.5	27.977	50	38
		5.0	27.431	24	43			3.0	34.666	36	40
12	5	1.5	40.506	50	38			4.5	46.346	>50	42
		3.0	27.695	32	40			6.0	55.766	>50	44
		4.0	20.272	50	41			7.5	65.469	>50	44
		5.0	17.050	>50	43			9.0	72.911	>50	45

At shallow depths, higher N-values are predicted as the electrodes are closely spaced resulting in higher apparent resistivity. As electrode separation increases, the current detected by potential electrodes diminishes, consequently reducing apparent resistivity with greater spacing. This relationship was utilized to develop the predictive N-value equations. However, this phenomenon is limited to low-density soils, and the predicted values overestimate the results by approximately three times the actual observed N-values. The predicted N-values demonstrate good accuracy in uniform soil layers, showing a better correlation with field observed values while maintaining conservative estimates below actual measurements for safety. Artificial Neural Networks (ANNs) are assessed to determine the capability of capturing complex, nonlinear patterns. The results showed that ANNs exhibited enhanced forecasting accuracy, especially when applied to diverse soil types with fine particle compositions whereas, linear analysis methods proved to be effective for homogeneous soil conditions, demonstrating that the choice of modelling approach should be tailored to the specific characteristics of the soil environment being studied. N-value interpretation permits soil density classification ranging from very loose to very dense, the uniform soil layers identified at the testing locations were determined to be very dense in nature. A simple mathematical equation was also developed from the ANN model for easy use in making predictions. However, the effectiveness of prediction model diminishes significantly in heterogeneous strata with varying soil properties. The relationship between depth and N-values represented in Figure 8 highlighted that LLM model performed well with experimental N-values using Wenner with R^3 of 0.9124.

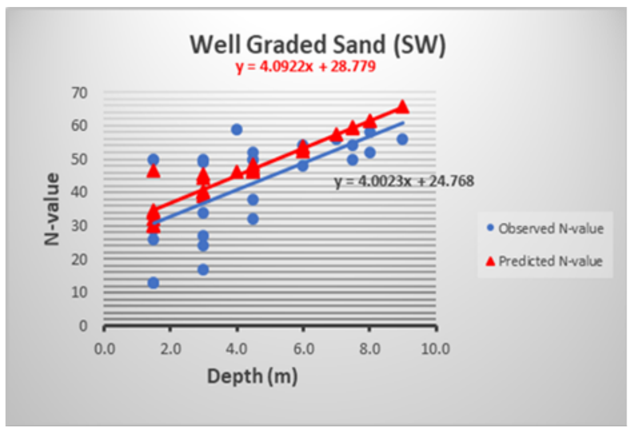

(a)

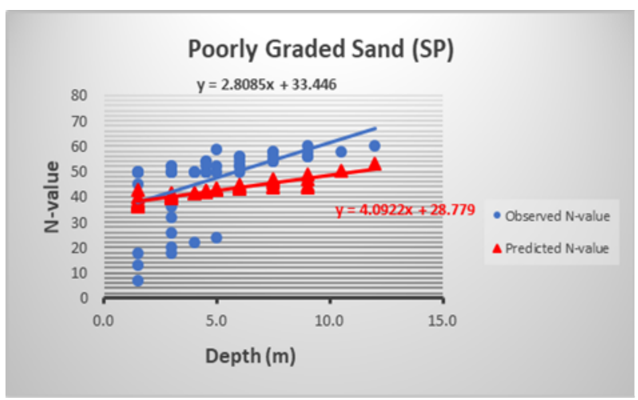

(b)

Fig 8. Observed and Predicted N-values of Well Graded Sand and Poorly Graded Sand

The comparison between N-values predicted by LLM and that obtained from borehole data along with Safe Bearing Capacity (SBC) calculated using **Eq.(7)** is presented in Table 5. There is no universal relationship between resistivity and SPT N value and specific correlations must be obtained for different locations. Work done by Braga et.al. (1999) was studied and found that the relationships developed by them can be utilized in areas with similar lithology. The work done by the authors represent sedimentary deposits consisting of claystones, sandy siltstones and clay siltstones with pockets of mudstone within the formation. Another study by Goncalves et. al. (2021) also emphasized that the areas chosen for their study contains quaternary deposits, clayey residual soils and siltstones clayey lenses. Their correlation is site specific and applicable to other soils having similar compositions and physical characteristics [4]. But the correlation equations developed in the present research is suitable for homogenous soil layers and for the particular type of soil considered in the study. Therefore, no direct comparison could be made between the correlations developed in the previous studies and those established in the present LLM-based study. While the derived correlation formulae are linear equations, subsequent studies may explore other mathematical models that account for multiple variables such as moisture content, relative density, and consistency parameters etc. It is also known that AI in the field of civil engineering has opened the door particularly in the utilization of machine learning (ML) techniques that finds solutions to complex engineering issues [24]. Artificial intelligence models are promisingly used, and Machine Learning models are one of the most efficient approaches in geotechnical engineering field [25]. While resistivity testing shows great potential for non-destructive soil classification and compaction assessment, limitations related to soil type specificity, environmental variability, and model generalizability exists [26].

Table 5. SBC from observed and predicted N-values

Sl. No.	Loca-tions	Depth (m)	Observed N-Value * (Experiment)	SBC from observed N-value (kN/m^2)	Predicted N- Value (LLM)	SBC from predicted N-value (kN/m^2)
1	2	4.5	50	318	46	289
2	3	4.5	50	318	42	263
3	3	6.0	>50	318	45	283
4	5	3.0	32	195	40	249
5	5	5.0	50	318	43	269
6	11	1.5	29	175	30	182
7	13	4.0	50	318	41	256
8	16	1.5	50	318	46	289
9	17	3.0	49	310	40	249
10	17	4.5	>50	318	47	296
11	19	3.0	36	222	40	249
12	19	4.5	50	318	42	263

(*All N values in the table greater than 50 are considered as 50 for SBC calculation)

Future recommendations include developing correlation equations that are not constrained by depth limitations. The scope should be expanded to encompass various soil types beyond the current research. Since this study concentrated on linear relationship correlations and highlighted moisture content as a critical factor in Electrical Resistivity Geophysical method, there is potential for creating non-linear equations that may better capture these complex relationships.

4 Conclusions

This study examined the effectiveness of electrical resistivity geophysical method using Wenner and Schlumberger arrays for subsoil investigation in the field. Prior to geophysical exploration, Wash boring and SPT tests were conducted. The following are the observations made from the present study.

- The Wenner array and Schlumberger array of electrical resistivity geophysical methods are useful in measuring the apparent resistivity of soils. Correlation equations developed using LLM to predict SPT-N values from electrical resistivity measurements showed high correlation with R^2 0.9124.
- The observed resistance values exhibited a decreasing trend from the soil surface in both the Wenner and Schlumberger arrays. In Schlumberger array, resistance values were higher than the Wenner array at the initial depth of 1.5m. However, beyond 1.5m the Wenner array showed higher resistance at all locations.
- The apparent resistivity ranged between 2.393Ωm and 246.176Ωm for well graded sand and for poorly graded sand, the resistivity ranges from 2.419Ωm to 125.600Ωm. Among the soils identified at different locations, sand showed higher range of resistivity compared to silt and clay. Higher apparent resistivity is due to the interlocked structure and compactness of sandy soil.
- Subsurface images interpolated into tomograms show variation in resistivity that revealed different strata. The apparent resistivity and true resistivity are the same in homogeneous layer.
- The presence of positive slope indicates that the moisture content increases with increase in depth from the ground level. It varied from 8.7% to 18.18% and 15.63% to 24.95% at locations 15 and 16 respectively representing positive slopes.

- Negative slope did not follow a definite pattern, it showed either an increase or decrease in its value, but the apparent resistivity showed increasing trend with respect to depth.
- Comparing observed and predicted SPT N values, both are in good agreement with comparable results at large depth, particularly when there is rebound of hammer with N greater than 50.
- The equations developed by LLM are well suited to predict SPT N obtained from Electrical resistivity values in homogeneous soil conditions. The limitation is that it is not applicable to mixed non-homogeneous/sedimentary layers.

5 Details of Ethical clearance

There are no potential conflicts of interest. This research did not involve any human participants and/or animals and informed consent is not applicable.

References

1) Sagar D, Dwivedi SB, Basudhar PK. Electrical Resistivity Tomography in Geotechnical Engineering Applications. Springer Singapore. 2021. https://dx.doi.org/10.1007/978-981-33-6346-5_14.
2) Braga AC, Malagutti FW, Dourado JC, Chang HK. Correlation of electrical resistivity and induced polarization data with geotechnical survey standard penetration test measurements. *Journal of Environmental and Engineering Geophysics*. 1999;4(2):123–130. https://doi.org/10.4133/JEEG4.2.123.
3) Roodposhti HR, Hafizi MK, Kermani MRS, Nik MRG. Electrical resistivity method for water content and compaction evaluation, a laboratory test on construction material. *Journal of Applied Geophysics*. 2019;168:49–58. https://doi.org/10.1016/j.jappgeo.2019.05.015.
4) Gonçalves JTD, Botelho MAB, Machado SL, Netto LG. Correlation between field electrical resistivity and geotechnical SPT blow counts at tropical soils in Brazil. *Environmental Challenges*. 2021;5:100220. https://doi.org/10.1016/j.envc.2021.100220.
5) Boualla O, Fadili A, Najib S, Mehdi K, Makan A, Zourarah B. Assessment of collapse dolines occurrence using electrical resistivity tomography: Case study of Moul El Bergui area, Western Morocco. *Journal of Applied Geophysics*. 2021;191:104366. https://doi.org/10.1016/j.jappgeo.2021.104366.
6) Bortolozo CA, Motta MFB, de Andrade MRM, Lavalle LVA, Mendes RM, Simões SJC, et al. Combined analysis of electrical and electromagnetic methods with geotechnical soundings and soil characterization as applied to a landslide study in Campos do Jordão City, Brazil. *Journal of Applied Geophysics*. 2019;161:1–14. https://doi.org/10.1016/j.jappgeo.2018.11.017.
7) Messe MRD, Kenfack JV, Ngapgue F, Wouatong ASL. Geotechnical soil mapping from electrical and mechanical properties: case study of the Bafoussam urban area, West Cameroon. *Applied Computing and Geosciences*. 2022;13:100078. https://doi.org/10.1016/j.acags.2021.100078.
8) Arora KR. Soil Mechanics and Foundation Engineering. Delhi, Nai Sarak, New Delhi. 2004. Available from: https://www.scribd.com/doc/242481857/SOIL-MECHANICS-AND-FOUNDATION-ENGINEERING-K-R-Arora-Delhi-2004-903p-pdf.
9) Prins C, Thuro K, Krautblatter M, Schulz R. Testing the effectiveness of an inverse Wenner-Schlumberger array for geoelectrical karst void reconnaissance, on the Swabian Alb high plain, new line Wendlingen–Ulm, southwestern Germany. *Engineering Geology*. 2019;249:71–76. https://doi.org/10.1016/j.enggeo.2018.12.014.
10) IS 15736:2007, Geological Exploration by Geophysical Method (Electrical Resistivity) - Code of Practice. New Delhi. 2007. Available from: https://law.resource.org/pub/in/bis/S14/is.15736.2007.pdf.
11) Hassan E, Rai JK, Anekwe UO. Geoelectrical Survey of Ground Water in Some Parts of Kebbi State Nigeria, a Case Study of Federal Polytechnic Bye-Pass Birnin Kebbi and Magoro Primary Health Center Fakai Local Government. *Geosciences*. 2017;7(5):141–149. https://doi.org/10.5923/j.geo.20170705.01.
12) Loke MH, Barker RD. Rapid least-square inversion of apparent resistivity pseudosections by a quasi-Newton method. *Geophysical Prospecting*. 1996;44(2):131–152. https://doi.org/10.1111/j.1365-2478.1996.tb00142.x?urlappend=%3Futm_source%3Dresearchgate.net%26utm_medium%3Darticle.
13) Nayak NV. Foundation Design Manual. New Delhi. 1996. Available from: https://www.scribd.com/document/188556502/NNARAYAN-v-nayaK-Foundation-Design-Manual.
14) Raiaan MAK, Mukta MSH, Fatema K, Fahad NM, Sakib S, Mim MMJ. A review on large language models: Architectures, applications, taxonomies, open issues and challenges. *IEEE Access*. 2024;12:26839–26874. https://doi.org/10.36227/techrxiv.24171183.v1.
15) Ducut JD, Alipio M, Go PJ, Concepcion RI, Vicerra RR, Bandala A, et al. A review of electrical resistivity tomography applications in underground imaging and object detection. *Displays*. 2022;73:102208. https://doi.org/10.1016/j.displa.2022.102208.
16) Yılmaz S, Narman C. 2-D electrical resistivity imaging for investigating an active landslide along a ridgeway in Burdur region, southern Turkey. *Arabian Journal of Geosciences*. 2015;8:3343–3349. https://doi.org/10.1007/s12517-014-1412-0.
17) Afshar A, Abedi M, Norouzi GH, Riahi MA. Geophysical investigation of underground water content zones using electrical resistivity tomography and ground penetrating radar: a case study in Hesarak-Karaj, Iran. *Engineering Geology*. 2015;196:183–193. https://doi.org/10.1016/j.enggeo.2015.07.022.
18) Ishak MF, Zolkepli MF, Masyhur EMH, Yunus NZM, Rashid ASA, Hezmi MA, et al. Interrelationship between borehole lithology and electrical resistivity for geotechnical site investigation. *Physics and Chemistry of the Earth, Parts A/B/C*. 2022;128:103279. https://doi.org/10.1016/j.pce.2022.103279.
19) Bertol VFNN, Kenfack JV, Kegni L, II HDTTB. Predicting soil parameters in Maroua 1st, Cameroon, using correlations of geophysical and geotechnical data. *Heliyon*. 2024;10(8):e29589–16. https://doi.org/10.1016/j.heliyon.2024.e29589.
20) Mirzaei L, Hafizi MK, Riahi MA. Application of Dipole–Dipole, Schlumberger, and Wenner–Schlumberger Arrays in Groundwater Exploration in Karst Areas Using Electrical Resistivity and IP Methods in a Semi-arid Area, Southwest Iran. *Water Resources in Arid Lands: Management and Sustainability*. 2021;p. 81–89. https://doi.org/10.1007/978-3-030-67028-3_7.
21) Water resources in arid lands: management and sustainability. In: Al-Maktoumi A, Abdalla O, Kacimov A, Zekri S, Chen M, Al-Hosni T, et al., editors. Springer International Publishing. 2021. https://doi.org/10.1007/978-3-030-67028-3.
22) Maio RD, Paola CD, Giovanni F, Piegari E, Pirone M, Santo A, et al. An integrated geological, geotechnical and geophysical approach to identify predisposing factors for flowslide occurrence. *Engineering Geology*. 2020;267:105473. https://doi.org/10.1016/j.enggeo.2019.105473.
23) Mohammed MA, Senosy MM, Abudeif AM. Derivation of empirical relationships between geotechnical parameters and resistivity using electrical resistivity tomography (ERT) and borehole data at Sohag University site, upper Egypt. *Journal of African Earth Sciences*. 2019;158:103563. https://doi.org/10.1016/j.jafrearsci.2019.103563.

24) Khan A, Khan M, Khan WA, Afridi MA, Naseem KA, Noreen A. Predicting pile bearing capacity using gene expression programming with SHapley Additive exPlanation interpretation. *Discover Civil Engineering*. 2025;2:58. https://doi.org/10.1007/s44290-025-00215-x.
25) Liu Y, Liang Y. Integrated machine learning for modeling bearing capacity of shallow foundations. *Scientific Reports*. 2024;14:8319. https://doi.org/10.1038/s41598-024-58534-5.
26) Kornkanok S, Puttiwongrak A, Inazumi S. Review of Correlations Between Soil Electrical Resistivity and Geotechnical Properties. *Geosciences*. 2025;15(5):166. https://doi.org/10.3390/geosciences15050166.